JOURNAL OF GEOPHYSICAL RESEARCH, VOL. 113, B03102, doi:10.1029/2007JB005135, 2008

Constraints on core-mantle electromagnetic coupling from torsional oscillation normal modes

M. Dumberry[1,2] and J. E. Mound[1]

Received 26 April 2007; revised 22 October 2007; accepted 7 December 2007; published 8 March 2008.

[1] Decadal axial angular momentum variations in the Earth's core are believed to be carried by the normal modes of torsional oscillations. Coupling with the mantle transfers angular momentum to the latter, leading to changes in length of day (LOD). Electromagnetic stresses at the core-mantle boundary (CMB) may be an important coupling mechanism as well as a source of dissipation for torsional oscillations. In this work, we investigate whether the observed spectra of fluid core velocities and LOD variations can be both explained in terms of the normal modes of torsional oscillations when the only coupling with the mantle is through electromagnetic stresses. We show that this explanation may be true when the magnetic field at the CMB is based on a downward continuation of surface observations, provided the conductance at the bottom of the mantle does not greatly exceed 10^8 S and small wavelength field features do not contribute more than approximately 25% of the total radial field at the CMB. A larger conductance or a higher amplitude radial magnetic field results in a damping of the normal modes of torsional oscillation that is sufficiently large that they should not be detectable. In particular, we show that this is the case for the conductance and radial magnetic field that are inferred from the Earth's forced nutations. If these constraints are correct, the decadal periodicities in the fluid velocity and LOD must then represent the preferred frequencies of the excitation mechanism of torsional oscillations rather than the signature of the free modes.

Citation: Dumberry, M., and J. E. Mound (2008), Constraints on core-mantle electromagnetic coupling from torsional oscillation normal modes, *J. Geophys. Res.*, *113*, B03102, doi:10.1029/2007JB005135.

1. Introduction

[2] Observed changes in the length of day (LOD) at decadal timescales are believed to be a consequence of an angular momentum exchange between the mantle and the core. Indeed, changes in the core angular momentum predicted on the basis of flows consistent with geomagnetic field variations are in agreement with those required to explain the changes in mantle angular momentum [*Jault et al.*, 1988; *Jackson et al.*, 1993]. The core flows that are involved in the decadal LOD changes likely consist of torsional oscillations, which are azimuthal oscillations of effectively rigid, cylindrical surfaces. Torsional oscillations are predicted by theory [*Taylor*, 1963; *Braginsky*, 1970], observed in geomagnetic field variations [*Zatman and Bloxham*, 1997; *Pais and Hulot*, 2000; *Hide et al.*, 2000] and it is on the basis of such flows that the core angular momentum is calculated.

[3] Furthermore, based on reasonable estimates of the magnetic field inside the core, the normal modes of torsional oscillations are predicted to have periods of decades [*Braginsky*, 1970]. The standard interpretation is then that the periodicities observed in the fluid velocity and LOD changes are caused by these free modes. In support of this hypothesis, time-dependent flows inverted from geomagnetic data appear to contain simple waves with characteristics that are compatible with free oscillations [*Zatman and Bloxham*, 1997; *Pais and Hulot*, 2000].

[4] Although there is a clear link between core flows and LOD, less is known about the mechanism, or the combination of mechanisms, by which angular momentum is exchanged within the core-mantle system. Proposed mechanisms of angular momentum transfer between the core and mantle include electromagnetic coupling [*Bullard et al.*, 1950; *Rochester*, 1960], topographic coupling [*Hide*, 1969; *Anufriyev and Braginsky*, 1977; *Jault and Le Mouël*, 1989], and gravitational coupling between the inner core and mantle [*Buffett*, 1996]. A recent approach to help discriminate between these different mechanisms has been developed by *Mound and Buffett* [2005] based on the assumption that the observed decadal, axisymmetric, equatorially symmetric, time-dependent core flows represent the normal modes of torsional oscillations. The authors investigated whether a given coupling mechanism allows the spectra of normal mode velocities and LOD changes to be simultaneously reproduced. They showed that electromagnetic coupling, by itself, does not appear capable of satis-

[1] School of Earth and Environment, University of Leeds, Leeds, UK.
[2] Presently at Department of Physics, University of Alberta, Edmonton, Canada.

0148-0227/08/2007JB005135$09.00

fying both constraints: when the coupling strength is low, not enough angular momentum is transferred to the mantle to explain the LOD changes; when the coupling strength is sufficiently large, the free modes of torsional oscillations should be rapidly attenuated.

[5] The strength of the electromagnetic coupling is proportional to the combination GB_r^2, where G is the conductance of the lower mantle and B_r the radial field across the CMB. For the free modes of torsional oscillations to explain both the LOD and flow velocities, *Mound and Buffett* [2005] concluded that the combination GB_r^2 must not be too large and that at least a second coupling mechanism must also be present. However, these conclusions were based on a simple formulation of the electromagnetic coupling, with the magnetic field at the core-mantle boundary (CMB) approximated as an axial dipole. Though an axial dipole may be an appropriate first order representation of the field in many situations, this is unlikely to be true when modeling the electromagnetic coupling between torsional oscillations and the mantle. Electromagnetic coupling results from the shearing of the radial magnetic field by azimuthal flow at the CMB. The radial component of an axial dipole field is maximum at the poles and zero at the equator, a geometry which is unfavorable for producing a strong net electromagnetic torque on the mantle. Indeed, the azimuthal flow associated with torsional oscillations must be zero at the poles, resulting in relatively little shear of the radial magnetic field at the latitudes where it is strongest under the axial dipole approximation. Furthermore, since the torque is integrated over the surface of the CMB, the net coupling is heavily weighted toward lower latitudes where the radial magnetic field, and therefore electromagnetic friction, of an axial dipole is weakest.

[6] A more realistic description of the magnetic field near the equatorial region could significantly enhance the torque for a given torsional oscillation flow. On the one hand, this makes it more likely that electromagnetic coupling by itself may be compatible with the spectra of LOD and fluid velocities. On the other hand, the enhanced coupling should lead to a more rapid attenuation of the free modes of torsional oscillations. A recent estimate based on the observed forced nutations of the Earth suggests a rather large value for GB_r^2 [*Buffett et al.*, 2002] and thus that electromagnetic coupling may indeed be rather large. If this is correct, the free modes of torsional oscillations may be damped very efficiently even if other coupling mechanisms participate. The observed decadal periodicities in the fluid velocity and LOD would then represent the preferred frequencies of the excitation mechanism of torsional oscillations, or ''forced'' torsional oscillations, rather than the free modes.

[7] The goal of this paper is to re-assess the role of electromagnetic coupling within the torsional oscillation normal mode approach. We develop expressions for the electromagnetic coupling that allows for a more complete description of the field at the CMB. We also show how the electromagnetic coupling associated with the higher degree components of the field can be approximated by a uniform radial field at the CMB. This permits an evaluation of the electromagnetic coupling that includes the effect of the unobservable, small length-scale features of the magnetic field at the CMB (which may contribute significantly to the amplitude of the radial field). With our more complete model for electromagnetic coupling, we show that it is possible to explain the fluid velocities and the changes in LOD in terms of the free modes of torsional oscillations solely from this coupling mechanism. However, we also confirm that if the combination GB_r^2 is as large as inferred by the forced nutations, the free modes of torsional oscillations should be rapidly attenuated.

2. Theory

[8] The electromagnetic torque that the fluid core exerts on the mantle can be written in terms of the surface integral of the electromagnetic stress at the CMB [*Rochester*, 1960; *Stix and Roberts*, 1984],

$$\mathbf{\Gamma} = -\frac{r_f^2}{\mu_o}\int_\Omega (\mathbf{r}\times\mathbf{B})B_r\, d\Omega, \tag{1}$$

where $\mathbf{B}$ is the magnetic field, B_r its radial component at the CMB ($r = r_f$), μ_o is the permeability of free space and Ω is the surface area of a unit sphere. The axial component of this torque is

$$\Gamma_z = -\frac{r_f^3}{\mu_o}\int_\Omega B_\phi B_r \sin\theta\, d\Omega, \tag{2}$$

where B_ϕ is the azimuthal component of the field. Changes in the magnetic field at the CMB lead to changes in Γ_z, which produces fluctuations in the rate of mantle rotation, i.e., changes in LOD. In this paper, we are interested in the magnetic field changes caused by the action of a horizontal flow near the CMB, namely torsional oscillations.

[9] In order to develop the appropriate mathematical expression for the torque it is useful to define the magnetic field in the core in terms of a poloidal-toroidal representation [e.g., *Gubbins and Roberts*, 1987],

$$\mathbf{B} = \nabla\times\nabla\times(S\mathbf{r}) + \nabla\times(T\mathbf{r}), \tag{3}$$

where S and T are scalars containing, respectively, the information on the poloidal and toroidal part of the field. According to this definition, the radial part of the field is entirely determined by the poloidal scalar S,

$$B_r = -\nabla^2(S\mathbf{r}) = \frac{\mathcal{L}^2 S}{r_f}, \tag{4}$$

where $\mathcal{L}$ is the angular momentum operator of quantum mechanics [e.g., *Edmonds*, 1960]. If we assume that the mantle is a perfect insulator, T must vanish at the CMB and the magnetic field in the mantle is a potential field described only in terms of S. The poloidal scalar field is related to the magnetic field measured at the Earth's surface ($r = r_a$) by

$$S = r_a\sum_{l,m}\frac{1}{l}\left(\frac{r_a}{r_f}\right)^{l+1}\left(g_l^m\cos m\phi + h_l^m\sin m\phi\right)P_l^m(\cos\theta), \tag{5}$$

where $P_l^m(\cos\theta)$ are associated Legendre polynomials and g_l^m and h_l^m are the familiar Gauss coefficients of the surface magnetic field. These coefficients are traditionally defined in terms of a Gauss-Schmidt normalization of real surface spherical harmonics,

$$\int_\Omega \left[P_l^m(\cos\theta)\right]^2 \left(\cos^2 m\phi,\ \sin^2 m\phi\right) d\Omega = \frac{4\pi}{2l+1}, \qquad (6)$$

and we follow this convention.

[10] We note that if the mantle were a perfect insulator, the electromagnetic torque would be identically zero. For a torque to occur, the mantle must necessarily have a non-zero conductivity in which case the approximation of the field at the CMB by (4)–(5) is not identically true. Observations of the forced nutations of the Earth suggest a relatively large conductivity in a thin layer at the bottom of the mantle [*Buffett*, 1992; *Buffett et al.*, 2002]. Indeed, we model electromagnetic coupling in this paper based on the assumption that such a layer is present. With a conducting layer at the bottom of the mantle, the toroidal part of the field need not vanish at the CMB and may be significant. However, it is assumed that the high-conductivity layer is sufficiently thin and the conductivity in the rest of the mantle small enough that the poloidal part of the field at the CMB is still described by (4)–(5).

[11] Flow in the core causes local changes in magnetic field by advection and shear. Advection of the field by torsional oscillations, a purely azimuthal flow, does not lead to a change in the torque at the CMB; the whole of the field is advected in the ϕ-direction, leading to an azimuthal rotation of the product $B_\phi B_r$ at a given latitude and no change in its integrated value along ϕ in (2). Only the changes in the magnetic field that are caused by shearing from torsional oscillations result in a change in the torque; this includes the shearing of the horizontal field by the horizontal gradients in the flow, and the shearing of the radial field by the velocity discontinuity at the CMB. It is generally assumed that the latter is much more important than the former [e.g., *Buffett*, 1992; *Holme*, 1998], an approximation that we adopt in this paper.

[12] Shearing from torsional oscillations leads to no change in the poloidal part of the field. Thus B_r and the poloidal part of B_ϕ are unaltered in (2), and the changes in the torque only involve the toroidal part of $B_\phi (= -\frac{\partial T}{\partial \theta})$. Consequently, the axial torque on the mantle can be written as [*Holme*, 1998]

$$\Gamma_z = \frac{r_f^3}{\mu_o} \int_\Omega \frac{\partial \tilde{T}}{\partial \theta} B_r \sin\theta \, d\Omega, \qquad (7)$$

where $\tilde{T}$ indicates the part of the toroidal scalar field produced by the shearing from torsional oscillations. The shear-induced toroidal field is obtained by solving the toroidal part of the diffusion equation in the mantle subject to boundary conditions at the CMB including continuity of the magnetic field and of the tangential electric field [*Stix and Roberts*, 1984]. When the conductivity $\sigma_m(r)$ is non-zero only in a thin layer of thickness $\Delta \ll r_f$ at the bottom of the mantle, and if one further assumes that the timescale of diffusion within that layer is short compared to the typical periods of torsional oscillations, the time-derivative part can be eliminated from the diffusion equation. When this is the case, *Holme* [1998] has shown that for a general tangential velocity $\mathbf{v}_H$ on the core side of the CMB, the solution for $\tilde{T}$ at the CMB is given by

$$\tilde{T} = -\mu_o G r_f \mathcal{L}^{-2}(\hat{r} \cdot \nabla_H \times B_r \mathbf{v}_H), \qquad (8)$$

where $\nabla_H = \nabla - \hat{\mathbf{r}}\partial/\partial r$ is the horizontal part of the gradient and G is the conductance of the layer determined by

$$G = \int_{r_f}^{r_f+\Delta} \sigma_m(r) dr. \qquad (9)$$

Given a radial magnetic field at the CMB and a conductivity profile in the mantle, the axial torque produced by torsional oscillations can be calculated from (7)–(9).

[13] We note that we do not take into account the back reaction of the Lorentz force on the flow. In general, this leads to a reduction of the overall torque. For radial field strength below 1 mT this represents a small correction [*Buffett et al.*, 2002], which we neglect here.

[14] In the *Mound and Buffett* [2005] formulation of the normal modes of torsional oscillations the fluid core is separated into a finite number of cylindrical shells. Therefore it is more convenient to write the electromagnetic torque in the form

$$\Gamma_z = \int_0^{r_f} \mathcal{F}_m(s)\left[u_f(s) - u_m\right] ds = \sum_j \mathcal{F}_m(s_j)\left[u_f(s_j) - u_m\right] \Delta s, \qquad (10)$$

where $s_j = r_f \sin\theta_j$ is the central radius of a cylindrical shell of finite thickness Δs, $u_f(s_j)$ is its rigid angular velocity and u_m is the angular velocity of the mantle [*Buffett*, 1998; *Mound and Buffett*, 2003, 2005]. In the appendix, we develop the mathematical expression for $\mathcal{F}_m(s_j)$ for an arbitrary magnetic field model at the CMB defined in terms of a set of Gauss coefficients as in (4)–(5). It is given by

$$\mathcal{F}_m(s_j) = \frac{r_f^5 G}{\Delta s} \boldsymbol{\alpha}^T \cdot \int_{\theta_1}^{\theta_2} \tilde{\mathbf{p}} \sin^2\theta d\theta, \qquad (11)$$

where the vector $\boldsymbol{\alpha}$ depends on the Gauss coefficients,

$$\theta_1 = \arcsin\left(\frac{s_j}{r_f} - \frac{\Delta s}{2r_f}\right), \qquad (12)$$

$$\theta_2 = \arcsin\left(\frac{s_j}{r_f} + \frac{\Delta s}{2r_f}\right), \qquad (13)$$

and the elements of vector $\tilde{\mathbf{p}}$ are

$$\tilde{p}_l = -\frac{2l+1}{l(l+1)}\left(\frac{\partial}{\partial\theta} P_l^0(\cos\theta)\right), \quad l = \text{odd}. \qquad (14)$$

[15] The expression for $\mathcal{F}_m$ given in (11) is different than the one used in the study of *Mound and Buffett* [2005]. In

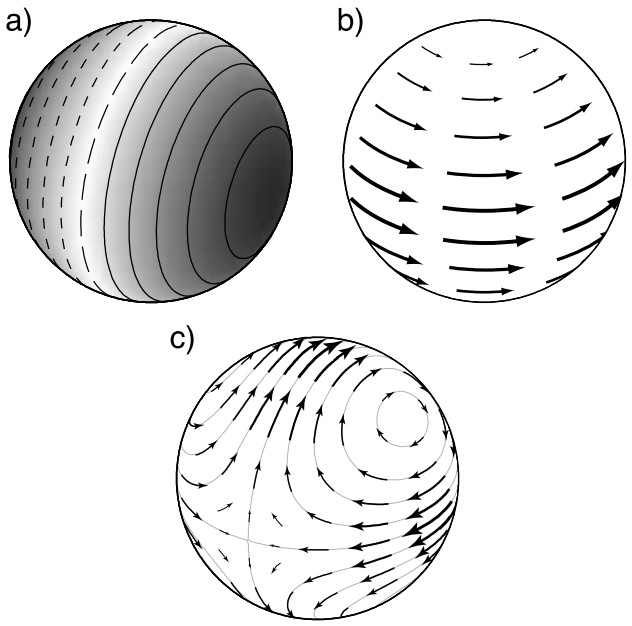

Figure 1. (a) Radial component of the magnetic field at the CMB given by (17). Grey scale indicates intensity, solid and dashed contours represent, respectively, outward and inward radial field. (b) Rigid azimuthal flow given by (18) is shown by arrows. (c) Toroidal magnetic field resulting from the shear of B_r by the flow. Grey lines represent the contours of the toroidal scalar T, and the arrows indicate the direction and intensity of the associated toroidal field. Large azimuthal fields are produced where B_r is maximum, but the requirement that the field lines be closed on spherical surfaces results in a non-zero toroidal field in places where B_r is minimum, i.e., at the poles for the example shown.

that study the radial field at the CMB was represented simply as an axial dipole. When B_r is axisymmetric, and when $\mathbf{v}_H = v_\phi \hat{\phi}$ is also axisymmetric, as is the case for torsional oscillations, one can show that the toroidal part of B_ϕ obtained from (8) is

$$B_\phi = -\frac{\partial \tilde{T}}{\partial \theta} = -\mu_o G B_r v_\phi, \tag{15}$$

an expression equivalent to that derived by *Buffett* [1998]. In this case, $\mathcal{F}_m$ simplifies to [*Buffett*, 1998]

$$\mathcal{F}_m(s) = 4\pi s^3 B_r^2 G\left(\frac{r_f}{z_f}\right), \tag{16}$$

where $z_f = \sqrt{r_f^2 - s^2}$; this is the expression for $\mathcal{F}_m$ used in *Mound and Buffett* [2005]. Although it is not immediately apparent, our more general expression in (11) is indeed equivalent to (16) when B_r is axisymmetric. However, for a more general field configuration that includes a non-axisymmetric part, (16) is no longer valid and the more general expression (11) must be used.

[16] The reason why equation (16) is inadequate when there are non-axisymmetric components is because (15) fails to account for the fact that the toroidal field lines produced by the shear of a non-axisymmetric B_r must be closed on spherical surfaces. This is most easily demonstrated with the help of a simple example. Consider a non-axisymmetric B_r described by the single Gauss coefficient g_1^1,

$$B_r = 2\left(\frac{r_a}{r_f}\right)^3 g_1^1 \sin\theta\cos\phi, \tag{17}$$

and a flow v_ϕ described by a simple rigid rotation

$$v_\phi = V_o \sin\theta. \tag{18}$$

Inserting (17) and (18) in (8), it can be verified that

$$\tilde{T} = -\frac{\mu_o G}{\sqrt{3}} g_1^1 V_o \left(\frac{r_a}{r_f}\right)^3 P_2^1(\cos\theta)\cos\phi, \tag{19}$$

and

$$\begin{aligned} B_\phi = -\frac{\partial \tilde{T}}{\partial \theta} &= \mu_o G V_o g_1^1 \left(\frac{r_a}{r_f}\right)^3 \cos\phi\left(-2\sin^2\theta + 1\right) \\ &= -\mu_o G B_r v_\phi + \frac{\mu_o G B_r v_\phi}{2\sin^2\theta}. \end{aligned} \tag{20}$$

[17] The first term on the right-hand side of (20) represents the part of B_ϕ arising directly from the shear of B_r, as in (15), and the second term represents the part of B_ϕ that arises because toroidal field lines must form closed contours on spherical surfaces. A visual representation of this is shown in Figure 1. When B_r is axisymmetric, B_ϕ is also axisymmetric; the toroidal field lines are purely azimuthal and form closed zonal contours. In this case (15) is valid and no correction term is required on the right-hand side of (20). However, for a field that also includes a non-axisymmetric part, (15) is invalid and the proper description for B_ϕ from (8) complicates the expression for $\mathcal{F}_m$ such that it no longer has the simple form of (16).

3. Influence of Field Geometry on the Torque

[18] The main difference between the results of this study and the results of *Mound and Buffett* [2005] arises from different assumptions about the geometry of the radial field at the CMB. To illustrate how the field geometry influences the electromagnetic coupling, we show in Figure 2 a comparison between $\mathcal{F}_m$ when the field is a simple axial dipole,

$$B_r^{(d)} = 2\left(\frac{r_a}{r_f}\right)^3 g_1^0 \cos\theta, \tag{21}$$

and $\mathcal{F}_m$ calculated from (11) for a field model that includes all spherical harmonics coefficients up to degree $l = 14$. The value of g_1^0 in (21) and of all Gauss coefficients in the full spectrum model are taken from the *gufm1* field model [*Jackson et al.*, 2000], time-averaged over the period 1950–1990. We designate these models as *gufm-ad* and *gufm-14*, respectively. The difference between these two cases is most notable near $s = r_f$ (the equator of the CMB) where the value of $\mathcal{F}_m$ for *gufm-ad* vanishes identically whereas that for *gufm-14* is maximum. At small s differences are much smaller, mainly because in *gufm-14* the part of the radial

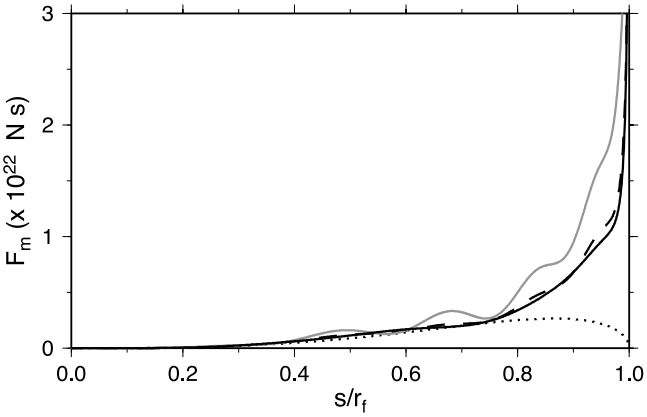

Figure 2. $\mathcal{F}_m$ as a function of s for various models of B_r at the CMB: *gufm-ad* (dotted line); *gufm-14* (black line); *gufm-30* (dashed line); *gufm-30flat* (grey line). See text for details of the field models. These results are based on a conductance of $G = 10^8$ S.

field from the axial dipole still dominates all other harmonics at high latitudes on the CMB. It is only when s is larger than about 0.8 r_f, corresponding to a latitude of approximately 35°, that the contribution to the radial field from coefficients other than g_1^0 becomes important.

[19] Features of the magnetic field at the CMB with a characteristic wavelength smaller than spherical harmonic degree 14 are not directly accessible from surface observations because they are masked by the crustal field. To test how small length-scale features may affect the torque we also show in Figure 2 a calculation of $\mathcal{F}_m$ for magnetic field models extrapolated to spherical harmonic degree $l = 30$. The Gauss coefficients for degrees $l = 1$ to $l = 14$ in the extrapolated models are the same as those of *gufm-14*. The coefficients with degrees $l = 15$ to $l = 30$ are determined based on the Lowes-Mauersberger power spectrum as a function of harmonic degree at the CMB [*Mauersberger*, 1956; *Lowes*, 1974],

$$R_l = (l+1)\left(\frac{r_a}{r_f}\right)^{2l+4} \sum_{m=0}^{l} \left(\left(g_l^m\right)^2 + \left(h_l^m\right)^2 \right). \tag{22}$$

[20] For one model we assume that $\log(R_l)$ decreases linearly with l, the slope being taken as the best fitting line between $l = 2$ and $l = 10$. The individual Gauss coefficients are set to a value given by this extrapolation with each coefficient multiplied by a random number taken from a normally distributed probability function with a zero mean and a standard deviation of 1. We refer to this model as *gufm-30*. As seen in Figure 2 the value of $\mathcal{F}_m$ resulting from such an extrapolation does not differ much from that of *gufm-14*, suggesting that the unobservable, small scale field in this specific case does not contribute significantly to the electromagnetic torque. However, this may not be true if the small scale field is stronger than suggested by the above extrapolation. To illustrate, we also present in Figure 2 a calculation of $\mathcal{F}_m$ for a second extrapolation, this one based on the assumption that R_l is constant for $l > 14$, the constant value being taken as the average value of R_l between $l = 2$ and $l = 10$. For this second extrapolation, which we refer to as *gufm-30flat*, $\mathcal{F}_m$ is visibly increased which shows that $\mathcal{F}_m$ may be significantly influenced by the small scale field.

[21] Since the unobservable small scale field may be important, it is desirable to seek a parameterization of its contribution to $\mathcal{F}_m$. One approach is to approximate the influence of the small scale field using an equivalent, uniform value of B_r at the CMB. We set this uniform field equal to the root mean square (RMS) amplitude of the radial component over the surface of the CMB, and denote it $\bar{B}_r$. Although the true radial field is non-axisymmetric, $\bar{B}_r$ is by definition axisymmetric. The variation of $\mathcal{F}_m$ expressed in terms of $\bar{B}_r$ should have a form similar to (16), except that, as explained above, the requirement that non-axisymmetric toroidal contours have to be closed should decrease the overall amplitude of the torque. Indeed, it can be verified that, if the radial field is contained in one single harmonic degree and that the energy is equally partitioned between all the Gauss coefficients of this degree, then $\mathcal{F}_m$ is given by

$$\mathcal{F}_m(s) = 2\pi s^3 \bar{B}_r{}^2 G\left(\frac{r_f}{z_f}\right), \tag{23}$$

exactly half of the prediction of (16). For a general multiharmonic radial field, the general trend of $\mathcal{F}_m$ is well captured by (23) so long as the Gauss coefficients with the same harmonic degree have comparable magnitudes. This is not the case for the Earth, as the axial dipole component is approximately an order of magnitude larger than all other components at the CMB. We find that, for an Earth-like full-spectrum field model at the CMB, $\mathcal{F}_m$ is well approximated by

$$\mathcal{F}_m(s) = 2\pi s^3 \left(\left(B_r^{(d)}\right)^2 + (\bar{B}_r)^2 \right) G\left(\frac{r_f}{z_f}\right), \tag{24}$$

where $B_r^{(d)}$ is given by (21) (it is a function of s) and $\bar{B}_r$ is the RMS of the total radial field (including the axial dipole term). The comparison between $\mathcal{F}_m$ calculated from (11) and its prediction from (24) is shown in Figure 3 for the *gufm-14* and *gufm-30flat* models. In both cases the general trend of $\mathcal{F}_m$ is well captured by (24), implying that $\mathcal{F}_m$ can be reasonably approximated by an axial dipole plus a monopole term that represents the combined effect of all coefficients of the field at the CMB.

[22] We note that, of the numerous random field model extrapolations that we have tested, the coefficients of model *gufm-30flat* are such that the departure of $\mathcal{F}_m(s)$ from (24) is comparatively large. This particular model was selected to show the extent of the largest expected deviation from (24). However, even in this case, (24) provides a good approximation to $\mathcal{F}_m(s)$.

[23] The representation of the torque by (24) is convenient because we do not need a detailed knowledge of the undetectable, small-scale structure of the field at the CMB. Therefore the exact form of the extrapolation of the field at the CMB beyond spherical harmonic degree 14 is not crucial. The important quantities for evaluating the electromagnetic coupling are the axial dipole strength and the overall RMS amplitude of the radial field. In particular, we consider an estimate of $\bar{B}_r = 0.69$ mT that has been suggested based on observations of Earth's forced nuta-

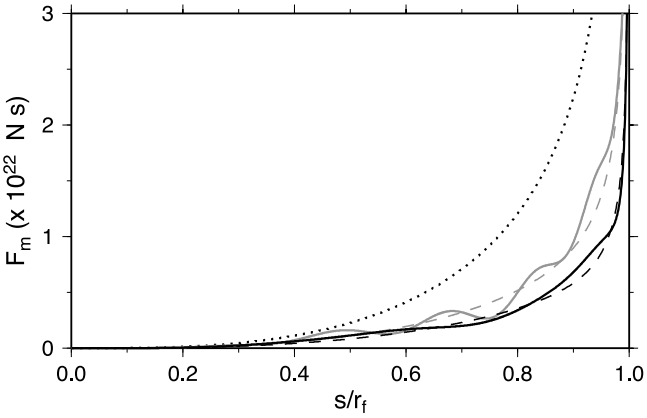

Figure 3. $\mathcal{F}_m$ as a function of s for the radial field model *gufm-14* (black line) and *gufm-30flat* (grey line), both calculated from (11), and the approximation from (24) for *gufm-14* (dashed black line) and *gufm-30flat* (dashed grey line). Also shown is $\mathcal{F}_m$ calculated from (24) for the radial field model MHB (dotted line). These results are based on a conductance of $G = 10^8$ S.

tions [*Buffett et al.*, 2002; *Mathews et al.*, 2002; *Mathews and Guo*, 2005]. Using (24), we can assess the implication of a radial field of that amplitude on $\mathcal{F}_m$. To do this we form a model of B_r at the CMB which comprises an effective monopole with amplitude 0.69 mT and an axial dipole equivalent to that of the *gufm-ad* model. We refer to this as the *MHB* model. We note that the value of $\bar{B}_r$ = 0.69 mT is well in excess of the value from *gufm-14* (0.319 mT), or even for the extrapolated model *gufm-30flat* (0.415 mT). Consequently, $\mathcal{F}_m$ should be significantly larger. This can be seen in Figure 3 where we show the calculation of $\mathcal{F}_m$ based on model *MHB* which indeed gives larger values of $\mathcal{F}_m$ than *gufm-14* or *gufm-30flat*.

4. Effects of Field Geometry and Amplitude on Torsional Oscillation Normal Modes

[24] In this section we investigate how different field geometries at the CMB influence the spatial and temporal behavior of torsional oscillation normal modes. The mathematical details and the numerical strategies used to investigate these modes are presented by *Mound and Buffett* [2005]. For all the calculations reported below, unless stated otherwise, we have used (11) to calculate the electromagnetic torque at the CMB for the *gufm*-based models, whereas we have used (24) for the MHB model. Torsional oscillations are also coupled electromagnetically to the inner core and the torque on the inner core is expressed as

$$\Gamma_z^{(icb)} = \int_0^{r_i} \mathcal{F}_i(s)\left[u_f(s) - u_i\right] ds, \tag{25}$$

where u_i is the angular velocity of the inner core. An expression for $\mathcal{F}_i$ can be derived in a similar manner as that for $\mathcal{F}_m$ in section 2. However, since we have little information on the field at the ICB and an expression of the form of (24) was shown to be a good approximation, in all calculations below we describe $\mathcal{F}_i$ simply as

$$\mathcal{F}_i(s) = 2\pi s^3 \left(\left(B_i^{(d)}\right)^2 + \left(\bar{B}_i\right)^2 \right) \hat{G}\left(\frac{r_f}{z_i}\right), \tag{26}$$

where $B_i^{(d)}$ and $\bar{B}_i$ refer to the axial dipole and RMS monopole components of the radial magnetic field at the ICB, and

$$\hat{G} = \frac{1}{4}(1 + i\,\mathrm{sgn}(\omega))\sigma_f \delta_f, \tag{27}$$

where σ_f is the conductivity of the fluid core (assumed equal to that of the inner core), $\delta_f = \sqrt{2/\omega\mu_o\sigma_f}$ is the skin depth in the fluid core, ω is the frequency of oscillation and $\mathrm{sgn}(\omega) = \omega/|\omega|$. The form of the coupling at the ICB is different than at the CMB, most notably from the appearance of a phase shift of $\frac{\pi}{4}$. This arises because, unlike within the thin conductive layer at the bottom of the mantle, the time-derivative term cannot be neglected in the diffusion equation in the inner core, and is instead approximated as $\partial/\partial t \rightarrow -i\omega$.

[25] The restoring force for torsional oscillation normal modes arises from the Lorentz force produced by shearing of the magnetic field perpendicular to the rotation axis (B_s). In the absence of coupling with the mantle and inner core the spatial and temporal behavior of the normal modes are determined by the details of B_s. Here, we have chosen a simple model of B_s with a constant value of 0.2 mT throughout the core. This amplitude was selected such that the period of the fundamental mode is approximately equal to 80 yr, consistent with the standard interpretation that LOD changes of the same period and shorter are due to angular momentum changes in the core carried by the free modes of torsional oscillations. The other physical parameters that enter our calculations are given in Table 1.

[26] We begin by considering the effect of the different magnetic field models at the CMB on the spatial structure of the normal modes. As seen in Figure 4 there is almost no difference between the spatial structures of the normal modes found using the *gufm-ad* and *gufm-30flat* models; the other *gufm* models also have very similar mode shapes. In all of these models the spatial structure of the normal modes is determined primarily by our chosen morphology of B_s, as is expected for free torsional oscillations. For model *MHB* the electromagnetic friction at the CMB sufficiently damps the normal modes to alter their spatial structure.

[27] The change in mode spatial structure can be best understood by considering the behavior of the fluid at $s = r_f$, i.e., at the equator of the CMB. For the axial dipole model $\mathcal{F}_m(s) \rightarrow 0$ as $s \rightarrow r_f$; therefore, this boundary acts as a free end and $\lim_{s \rightarrow r_f} \partial u_f/\partial s = 0$. (Note that the boundary condition at $s = 0$ also results in a free end.) If the magnetic field is not a pure axial dipole, then the CMB electromagnetic coupling will not, in general, be zero at $s = r_f$. For a sufficiently strong coupling at the equator of the CMB the boundary would act as a fixed end such that $u_f = 0$ and $\partial u_f/\partial s$ is maximum at $s = r_f$. In the former case the characteristic length-scale of the nth mode $L_{free} \propto 2(r_f - r_i)/n$; in the latter case the characteristic length-scale of the nth mode is $L_{fixed} \propto 2(r_f - r_i)/$

Table 1. Physical Parameters Used in the Models

Parameter	Symbol	Value
Radius of ICB	r_i	1.22×10^6 m
Radius of CMB	r_f	3.48×10^6 m
Density of fluid core	ρ	1.2×10^4 kg m^{-3}
Inner core moment of inertia	C_i	5.87×10^{34} kg m^2
Mantle moment of inertia	C_m	7.12×10^{37} kg m^2
Core conductivity	σ_f	5×10^5 S m^{-1}
Conductance of lowermost mantle	G	10^8 S
Radial magnetic field		
Cylindrically in fluid	B_s	0.2 mT
RMS of axial dipole at ICB	$\bar{B}_i^{(d)}$	2.0 mT
RMS monopole at ICB	$\bar{B}_i$	3.0 mT
RMS of MHB dipole at CMB	$\bar{B}_r^{(d)}$	0.226 mT
MHB monopole at CMB	$\bar{B}_r$	0.69 mT

($n - 0.5$). Increasing the electromagnetic coupling near the equator of the CMB moves the model toward the fixed end boundary condition, as reflected by the longer wavelengths and non-zero value of $\partial u_f/\partial s$ for the modes of the *MHB* model. For the *gufm* based models containing higher order field components the strength of the coupling is largest near $s = r_f$ (Figure 2), but the overall amplitude of the coupling remains too small to significantly alter the shape of the modes. The derivative of u_f at $s = r_f$ is non-zero for *gufm-30flat*, but it is not sufficiently large to be obvious on the scale of Figure 4.

[28] The structure of the modes shown in Figure 4 would be different had we selected a different profile of B_s as a function of s. When the amplitude of B_s varies with s, the general tendency is for the spatial wave number to increase in regions of weaker B_s. For instance, using a perhaps more realistic profile where B_s decreases with s, the angular velocity variations would have been more concentrated toward $s = r_f$.

[29] The dissipation associated with electromagnetic coupling affects the temporal behavior of the normal modes. In Figure 5 we plot the period and decay times of all normal modes having periods greater than ten years. Model *gufm-ad* has decadal period normal modes whose decay times are greater than one hundred years. Including the higher order components in the *gufm* models shortens the decay times relative to the axial dipole case; the accompanying increases in mode periods are small (reaching 4% for the lowest harmonic of model *gufm-30flat*). Models *gufm-14* and *gufm-30* have torsional oscillation normal modes with very similar periods and decay times, in both cases the period of the lowest harmonic is approximately equal to its decay time. The temporal behavior of the gravest modes in these two models are also broadly consistent with observations [*Zatman and Bloxham*, 1997].

[30] An increase in the amplitude of the RMS radial field leads to enhanced dissipation and more rapid decay times for the modes. For model *gufm-30flat* the dissipation is sufficiently large that the lowest harmonic has a decay time shorter than its period; however, the remainder of this model's torsional oscillation normal modes have decay times greater than their periods. The large monopole component in model *MHB* greatly reduces the decay times of the modes; the mode periods are also increased with this effect being greatest for the lower harmonics (the period of the lowest harmonic is 24% longer than the equivalent mode in *gufm-ad*). The five gravest modes of model MHB have decay times shorter than their periods.

[31] It is important to stress that the more rapid decay times of model *MHB* is due to the larger $\bar{B}_r$ compared to other models; it is not an unintended consequence of using (24) to approximate the coupling at the CMB. In fact, compared to a full spectrum field, the dipole-monopole approximation of (24) tends to underestimate the dissipation of the normal modes. This is illustrated in Figure 5, where the decay times of model *gufm-14* when $\mathcal{F}_m(s)$ is calculated using (24) are larger than those when using (11).

[32] The increased dissipation in the presence of a larger $\bar{B}_r$ can be further understood with the following considerations. *Holme* [1998b] showed that for an axial dipole field, the rate of dissipation of angular momentum in the core is proportional to the angular momentum itself. This is because the angular momentum of the core is given by

$$L = \rho r_f^4 \int_\Omega u_\phi \cos^2\theta \sin\theta d\Omega = \frac{8\pi}{15}\rho r_f^4 \left(t_1^0 + \frac{12}{7}t_3^0\right), \qquad (28)$$

where ρ is density and the t_l^0 are spherical harmonic coefficients of the flow (see equations (A9)–(A10)), and the same integral is involved in the electromagnetic torque on the mantle

$$\Gamma_z = 3r_f^3 G\left(\bar{B}_r^{(d)}\right)^2 \int_\Omega u_\phi \cos^2\theta \sin\theta \, d\Omega, \qquad (29)$$

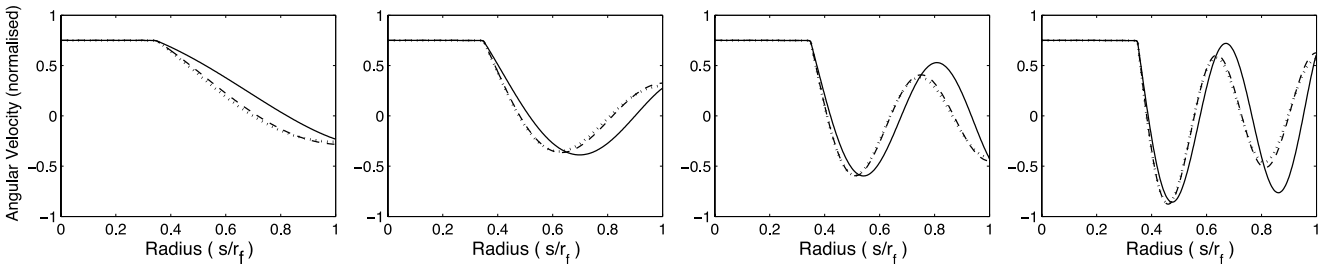

Figure 4. Angular velocity plotted against cylindrical radius for the first four torsional oscillation normal modes of the *gufm-ad* (dotted lines), *gufm-30flat* (dashed lines) and *MHB* (solid lines) magnetic field models. The modes are normalized so that all modes have the same angular velocity at $s = 0$. Other physical parameters are given in Table 1.

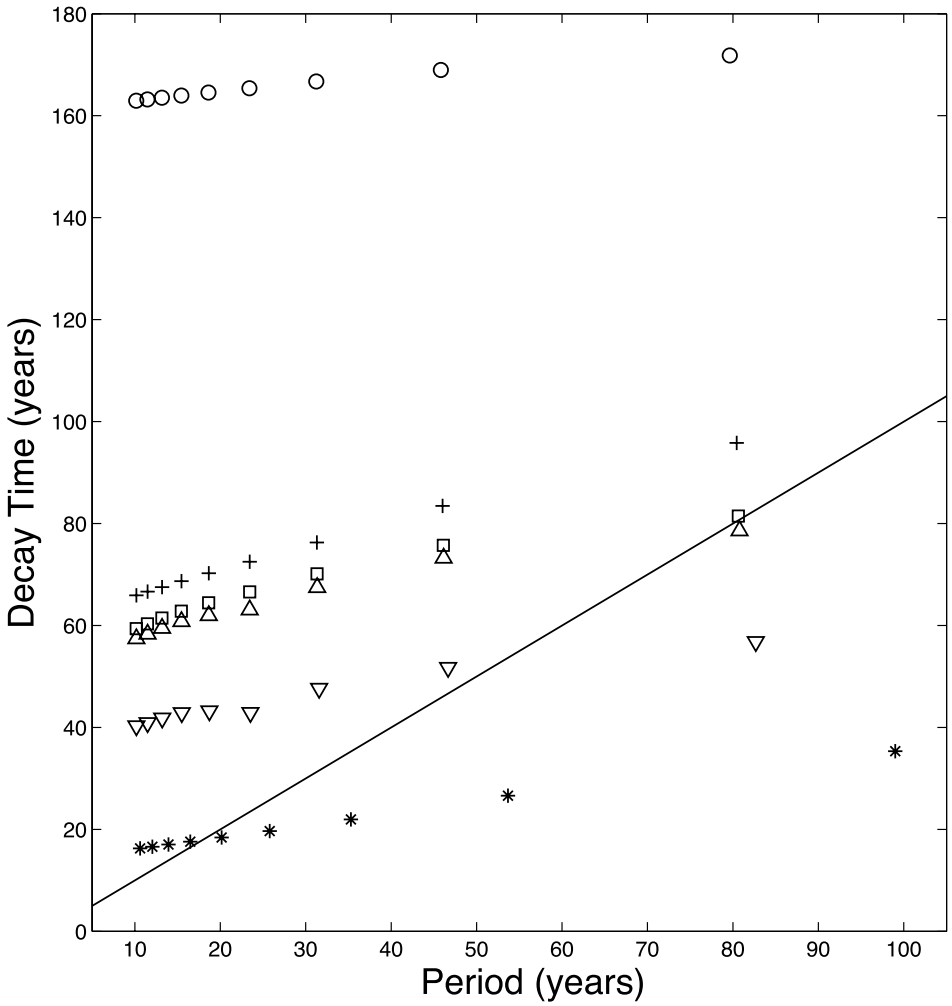

Figure 5. Decay time of the torsional oscillation normal modes plotted versus their period. Different symbols correspond to different magnetic field models at the CMB: *gufm-ad* (circles), *gufm-14* (squares), *gufm-30* (upward-pointed triangles), *gufm-30flat* (downward-pointed triangles) and *MHB* (asterisks). The + symbols are for *gufm-14* but using (24) instead of (11). The solid line indicates where decay time is equal to period. Only modes with periods greater than 10 years are plotted. Other physical parameters are given in Table 1.

where $\bar{B}_r^{(d)} = (2/\sqrt{3})\,(r_a/r_f)^3\, g_1^0$ is the RMS amplitude of the axial dipole field. Since the torque on the mantle is equal and opposite to the torque on the core, the angular momentum in the core must follow

$$\frac{dL}{dt} = -\frac{L}{\tau_d} + f(t), \tag{30}$$

where $f(t)$ contains other contributions to the torque, and where

$$\tau_d = \frac{\rho\, r_f}{3G\left(\bar{B}_r^{(d)}\right)^2}. \tag{31}$$

Equation (30) shows that electromagnetic coupling causes angular momentum to decay exponentially with a typical timescale τ_d. As noted by *Holme* [1998b], only the flow harmonics t_1^0 and t_3^0 are directly attenuated by electromagnetic coupling with an axial dipole field. However, because the normal modes of torsional oscillations also involve higher flow harmonics (see Figure 4), and because the different flow harmonics are coupled through B_s, the dissipation of t_1^0 and t_3^0 leads to an indirect dissipation of all flow harmonics. It is based on the large dissipation of free torsional oscillations predicted by (31) that *Holme* [2000] argued against a large deep-mantle conductivity under the Pacific, as had been suggested by *Runcorn* [1955] to explain the lower geomagnetic secular variation observed historically in this region of the CMB.

[33] The above ideas can be extended to a more general field representation. When the magnetic field is approximated by a monopole field, we can write the electromagnetic torque on the mantle as

$$\Gamma_z = \frac{1}{2} r_f^3 G(\bar{B}_r)^2 \int_\Omega u_\phi \sin\theta d\Omega = \frac{8\pi}{6} r_f^3 G(\bar{B}_r)^2 t_1^0, \tag{32}$$

where the factor 1/2 captures the effect of the non-axisymmetric part of the field on the torque, as in (23). The only harmonic of the flow that is coupled directly to a monopole field is t_1^0. For a field approximated by a dipole and a monopole, unlike for the purely dipolar case, we cannot build a simple equation for the evolution of the angular momentum in the core, except if $t_3^0 = 0$, in which case

$$\frac{dL}{dt} = -\frac{L}{\tau} + f(t), \tag{33}$$

where

$$\tau = \left(\frac{1}{\tau_d} + \frac{1}{\tau_m}\right)^{-1}, \tag{34}$$

and

$$\tau_m = \frac{2\rho r_f}{5G(\bar{B}_r)^2}. \tag{35}$$

[34] The decay times of the normal modes of torsional oscillations for a general field at the CMB can thus be approximated by (35). This is obviously a simplification because t_3^0 has been neglected from (33) and because we have not considered the internal coupling that leads to the indirect dissipation of other flow harmonics. In addition, using the true spectrum of the field instead of a monopole, not only t_1^0 is directly involved in the CMB coupling in (32), but higher flow harmonics are as well. This would enhance dissipation, as illustrated by the shorter decay times of model *gufm-14* in Figure 5 when we use (11) versus when we use (24). Nevertheless, compared to the case of a simple axial dipole field, the decrease in the decay times of the modes can be measured by the ratio

$$\frac{\tau_d}{\tau} = 1 + \frac{\tau_d}{\tau_m}. \tag{36}$$

[35] Comparing models *gufm-ad* ($\bar{B}_r^{(d)} = 0.226$ mT) and MHB ($\bar{B}_r = 0.69$ mT), we obtain $\tau_d/\tau_m \approx 7.8$, which gives $\tau_d/\tau \approx 8.8$, the approximate ratio between the decay times of the modes of these two models (Figure 5).

[36] The constant B_s that we have adopted here is sufficient to demonstrate how different models of the radial field at the CMB influence electromagnetic coupling and affect the dissipation of the normal modes. However, the precise periods and decay times of the modes are dependent on the selected profile of B_s as a function of s. Using a model of B_s that decreases with s, a likely more realistic profile, dissipation is increased and the normal modes are more attenuated. The decay times of the modes for each of the CMB field models plotted in Figure 5 would be smaller. The main factor controlling the period of the modes is the amplitude of B_s. With a larger amplitude, the modes shown in Figure 5 would have shorter periods. Thus for any choice of CMB field model, whether the gravest modes are heavily attenuated (i.e., periods longer than decay times) depends on the geometry and amplitude of B_s. For instance, by selecting a larger amplitude than $B_s = 0.2$ mT, it would have been possible for all of the free modes associated with model MHB to have decay times larger than their periods. Of course, the period of the fundamental mode in this case would be smaller than approximately 10 yr. In summary, our results suggest that with a CMB field amplitude as large as in the *MHB* model, all modes with periods of approximately 10 yr or larger are heavily damped, though exactly how many modes this corresponds to depends on the amplitude and geometry of B_s. Free torsional oscillations with periods of 10 yr or larger are incompatible with a radial magnetic field at the CMB as large as suggested by the forced nutations.

5. Constraints on Electromagnetic Coupling From Observed Flow Velocities and Changes in LOD

[37] Changes in LOD with magnitudes of 1–3 ms on decadal timescales are generally assumed to represent the normal modes of torsional oscillations of the core. Indeed, although continuous excitation of an over-damped system cannot be ruled out, the fluid motion appears to consist of damped waves with amplitudes of a few tenths of mm/s and periods of several decades [*Jault et al.*, 1988; *Jackson et al.*, 1993; *Zatman and Bloxham*, 1997; *Pais and Hulot*, 2000; *Hide et al.*, 2000]. If this is correct, the coupling mechanism between the core and the mantle must then allow free modes of torsional oscillations with this magnitude to transfer sufficient angular momentum to explain the observed LOD variations. We now investigate whether electromagnetic coupling, by itself, is consistent with these requirements. To do this, we calculate the response of the torsional oscillation normal modes model of *Mound and Buffett* [2005] to an imposed excitation. We consider a forcing that represents excitation of torsional oscillations due to convective motion in the fluid core containing power over a broad range of wavelengths and frequencies (the particular form of the forcing used is given by *Mound and Buffett* [2005]). Spectra of fluid velocity and LOD change for the *gufm-ad*, *gufm-14* and MHB field models for $G = 10^8$ S are show in Figure 6. In all cases the amplitude of the applied forcing was 5×10^{18} N m.

[38] For the *gufm-ad* model we find that fluid velocities of the order of the observations are excited by the chosen forcing; additionally, there are distinct peaks in the spectrum which are associated with the torsional oscillation normal modes. However, for this magnetic field model the net electromagnetic coupling at the CMB does not produce sufficient torque to excite the observed level of LOD change; the electromagnetic torque associated with the axial dipole component of the magnetic field plays a relatively small role in the transfer of angular momentum between the core and mantle on periods of several decades.

[39] The large monopole in the *MHB* results in a larger electromagnetic coupling. As can be seen on Figure 6, the larger transfer of angular momentum to the mantle results in larger changes in LOD, to the level of the observed variations. However, the larger electromagnetic coupling also results in a more heavy damping which has reduced the fluid velocity below 0.1 mm/s. There are no spectral peaks associated with the long period torsional oscillation normal modes since their decay times are much less than their periods (recall Figure 5). For this case, electromagnetic

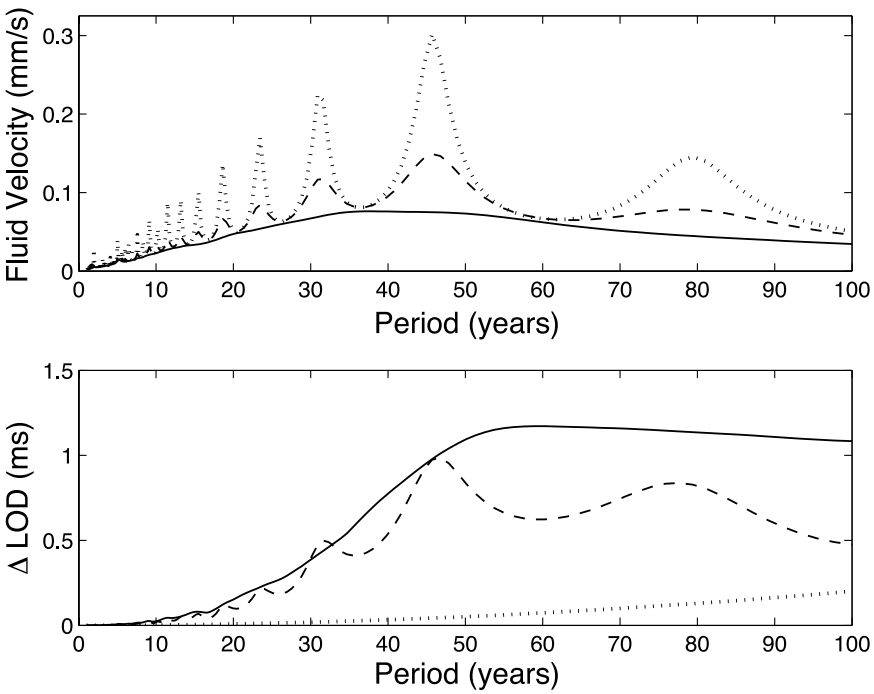

Figure 6. Spectra of fluid velocity (top) and change in length of day (bottom) for the prescribed forcing. Results are given for the *gufm-ad* (dotted lines), *gufm-14* (dashed lines) and *MHB* (solid lines) magnetic field models. Other physical parameters are given in Table 1.

damping is sufficiently large that the free modes of torsional oscillations would not be detectable.

[40] When the overall RMS radial field at the CMB is smaller, as is the case for the *gufm-14* model, there is less dissipation. Although the fluid velocities excited by the chosen forcing are smaller for model *gufm-14* than for *gufm-ad*, the spectral peaks associated with the torsional oscillation normal modes are still present, albeit less pronounced (Figure 6). The peak associated with the lowest harmonic is almost absent since the decay time and period of this mode are nearly equal; however, the other modes have decay times well in excess of their periods (recall Figure 5). Although the fluid velocities are lower for the *gufm-14* model than for *gufm-ad*, the associated changes in LOD are larger. In fact, the amplitude of LOD oscillations are nearly as large as the observed decadal LOD variations and by slightly increasing the amplitude of the applied forcing both the observed LOD and fluid velocity amplitudes can be matched; similar results are obtained using the *gufm-30* and *gufm-30flat* magnetic models. Therefore we find that magnetic field models derived from the downward continuation of surface measurements can produce a net electromagnetic coupling which is consistent with the observed dynamics of axial angular momentum transfer between the core and mantle on decadal timescales.

[41] The above results (and indeed all the results presented on Figures 2 to 6) apply for a conducting layer with an assumed conductance of $G = 10^8$ S. As can be seen from equations (11) or (24), $\mathcal{F}_m$ is proportional to the combination $G(\bar{B}_r)^2$. This implies that similar results as those presented above could have been obtained by keeping a fixed value of $\bar{B}_r$ but varying G. Hence though the *gufm-14* model can explain both the LOD and fluid velocity spectra through electromagnetic coupling, this is only true provided the conductance is not much larger than 10^8 S.

[42] The electromagnetic coupling involved in the forced nutations similarly provides a constraint on the combination $G(\bar{B}_r)^2$. The estimate of $\bar{B}_r = 0.69$ mT is derived based on a conductance of $G = 10^8$ S [*Buffett et al.*, 2002]. A lower value of G would imply a larger estimate of $\bar{B}_r$ and vice versa, and no change in the spectra of model MHB in Figure 6. Therefore the constraints derived from the forced nutations are incompatible with unattenuated torsional oscillation normal modes.

6. Discussion and Conclusion

[43] We have shown how a realistic model of the magnetic field at the CMB can be incorporated into the electromagnetic torque that enters the formalism of torsional oscillation normal modes. We have also shown that this torque can be approximated as that resulting from an axial dipole plus a constant radial field. This allows the unobservable, small scale part of the field at the CMB to be taken into account in the electromagnetic coupling. Previous work on torsional oscillation normal modes which did not include a complete description of the CMB magnetic field found that electromagnetic coupling alone cannot account for observations of both core fluid velocity and LOD changes [*Mound and Buffett*, 2005]. In contrast, we find that CMB magnetic field models based on *gufm1* [*Jackson et al.*, 2000] can produce an electromagnetic coupling that is compatible with observational constraints on angular momentum transfer between the core and mantle at decadal periods, a result consistent with that of *Holme* [1998b]. This is provided the conductance at the base of the mantle does not greatly exceed $G = 10^8$ S.

[44] For a larger conductance, or if the small wavelength features contribute significantly to the total radial magnetic field at the CMB, the stronger electromagnetic coupling results in over-damped torsional oscillation normal modes. Though angular momentum is transferred between the core and mantle, no decadal spectral peaks are generated in the LOD changes and fluid velocity. We found that this is the case when we use the conductance and RMS radial magnetic field strength derived from the forced nutation studies (10^8 S and 0.69 mT, respectively). Periodicities in observed changes in LOD and fluid core motions are generally interpreted as the expression of under-damped torsional oscillation normal modes. However, if the constraints from the nutations are correct, free modes of torsional oscillations should rapidly decay. This would imply that the observed decadal periodicities in torsional oscillations and LOD variations must reflect preferred frequencies in the excitation mechanism rather than the frequencies of free modes.

[45] Our results have been derived with electromagnetic coupling acting as the sole mechanism for angular momentum transfer between the core and the mantle. Other mechanisms can participate in this transfer of angular momentum, most notably topographic coupling at the CMB [*Hide*, 1969; *Anufriyev and Braginsky*, 1977; *Jault and Le Mouël*, 1989] and gravitational coupling between the mantle and the inner core [*Buffett*, 1996, 1998; *Mound and Buffett*, 2003]. The latter mechanism has been shown to be compatible, by itself, with free torsional oscillations and the LOD changes [*Mound and Buffett*, 2005]. However, a large electromagnetic coupling nevertheless results in rapid damping of the normal modes of torsional oscillations even when inner core-mantle gravitational coupling or other coupling mechanisms are present.

[46] We note that the dissipation required to explain the observations of forced nutations can also be explained in terms of viscous coupling if the effective viscosity in the core (or at least in a boundary layer at the top of the core) is much larger than typical estimates of its molecular value [*Palmer and Smylie*, 2005; *Mathews and Guo*, 2005; *Deleplace and Cardin*, 2006]. However, adopting a similar scenario in our study would not alter our conclusions: though electromagnetic damping would be much lower, viscous coupling would be elevated to such a level that a similar damping of the free modes of torsional oscillations would occur.

[47] If the standard interpretation that observed decadal rigid cylindrical motions in the core represent the normal modes of torsional oscillations is correct, then our results can be used to constrain the conductance and overall radial field strength at the CMB. As is the case for the nutation studies, we obtain a constraint on the combination of G and $(\bar{B}_r)^2$ rather than individual constraints on each of these quantities. If we require that all normal modes have decay times greater than their periods, then with, $G = 10^8$ S, model *gufm-14* is only just compatible with this constraint (Figure 5). With $\bar{B}_r = 0.32$ mT for this model, this suggests an upper bound for $G(\bar{B}_r)^2$ of approximately 10 N m^{-3} s. This constraint is likely too severe as model *gufm-30flat*, which has $\bar{B}_r = 0.415$ mT, produces fluid velocity and LOD spectra similar to those shown for model *gufm-14* in Figure 6. The upper bound for $G(\bar{B}_r)^2$ is then closer to 20 N m^{-3} s. Another consideration is that the periods and decay times of the normal modes depend strongly on the radial magnetic field within the fluid core and we have considered only one, very simple, model of B_s. If electromagnetic coupling at the equator of the CMB is large, then models in which B_s decreases as $s \rightarrow r_f$ tend to have greater dissipation than equivalent models with a constant B_s; such variable B_s models would lead to a more restrictive upper bound on $G(\bar{B}_r)^2$. A firm limit requires more information about the magnetic field within the core. It is not possible to obtain information about the unobservable high-order components of the field at the CMB without an a priori assumption of the conductance of the lower mantle. Assuming a value of $G = 10^8$ S, our constraint implies that field features with spherical harmonic beyond degree 14 do not contribute more than approximately 25% of the total radial field at the CMB.

[48] If one accepts the value of $G(\bar{B}_r)^2 = 47$ N m^{-3} s derived from studies of the forced nutations, then the observed decadal rigid cylindrical motions in the core cannot represent the normal modes of torsional oscillations. Instead, these would have to represent the forced cylindrical motions, or forced torsional oscillations, excited by the underlying convective dynamics in the core.

Appendix A: Axial Torque at the CMB

[49] The axial component of the torque at the CMB is (see equation (2))

$$\Gamma_z = -\frac{r_f^3}{\mu_o}\int_\Omega B_\phi B_r \sin\theta \, d\Omega, \tag{A1}$$

where B_r and B_ϕ are, respectively, the radial and azimuthal components of the magnetic field at the CMB (of mean radius r_f), μ_o is the permeability of free space, and Ω is the surface area of a unit sphere. Since B_ϕ comprises both a poloidal and toroidal part, the torque can be conveniently separated into poloidal and toroidal components. Here, we are interested in the torque that results from tangential fluid motions at the CMB, and we broadly follow the derivation presented by *Holme* [1998]. Tangential fluid motions only affect the toroidal part of $B_\phi (= -\frac{\partial T}{\partial \theta})$, and consequently we are only concerned with the toroidal part of the torque, which is written as

$$\Gamma_z = \frac{r_f^3}{\mu_o}\int_\Omega \frac{\partial T}{\partial \theta} B_r \sin\theta \, d\Omega. \tag{A2}$$

Integrating by parts once, we can rewrite the above expression as

$$\Gamma_z = -\frac{r_f^3}{\mu_o}\int_\Omega T\left(\frac{\partial B_r}{\partial \theta}\sin\theta + 2B_r\cos\theta\right) d\Omega. \tag{A3}$$

The toroidal scalar T at the CMB resulting from a tangential velocity jump at the CMB $\mathbf{v}_H$ is,

$$T(r_f) = -\mu_o G r_f \mathcal{L}^{-2}(\hat{\mathbf{r}} \cdot \nabla_H \times B_r \mathbf{v}_H), \tag{A4}$$

where $\nabla_H = \nabla - \hat{\mathbf{r}}\partial/\partial r$ is the horizontal part of the gradient, and G is the conductance of a layer of thickness Δ

with conductivity $\sigma_m(r)$ at the bottom of the mantle and is defined by (9). Substituting (A4) in (A3) we get

$$\Gamma_z = r_f^4 G \int_\Omega \left(\mathcal{L}^{-2}\mathcal{Q}\right)\mathcal{K} d\Omega, \tag{A5}$$

where

$$\mathcal{Q} = \hat{\mathbf{r}} \cdot \nabla_H \times B_r \mathbf{v}_H, \tag{A6}$$

$$\mathcal{K} = \frac{\partial B_r}{\partial \theta} \sin\theta + 2B_r \cos\theta. \tag{A7}$$

[50] We calculate the torque integral in (A5) by spherical transform, and expand both $\mathcal{Q}$ and $\mathcal{K}$ in spherical harmonics. Since the orthogonality rules for spherical harmonics are such that the integral (A5) is non-zero only for the coefficients of $\mathcal{Q}$ and $\mathcal{K}$ of equal degree and order, the operator $\mathcal{L}^{-2}$ can be applied interchangeably to either without affecting the end result. Because $\mathcal{K}$ is linearly related to B_r and the latter involves a $\mathcal{L}^2$ term (see equation (4)), it is mathematically more convenient to apply $\mathcal{L}^{-2}$ to $\mathcal{K}$. The torque in (A5) can be written in the following general form,

$$\Gamma_z = r_f^4 G \mathbf{k}^T \cdot \mathbf{q}, \tag{A8}$$

where the vectors $\mathbf{k}$ and $\mathbf{q}$ contain the coefficients of the spherical expansion of $\mathcal{L}^{-2}\mathcal{K}$ and $\mathcal{Q}$, respectively. Elements of the vector $\mathbf{k}$ are determined following the method detailed by *Holme* [1998], whereas the elements of $\mathbf{q}$ can be obtained by spherical transform. Both vectors contain the Gauss coefficients of the magnetic field as defined in (4)–(5).

[51] For our purpose, we need to express the torque in terms of torsional oscillations, in which case $\mathbf{v}_H$ in (A6) is $\mathbf{v}_\phi$, where $\mathbf{v}_\phi$ is both axisymmetric and symmetric about the equator. We can thus write it as

$$\mathbf{v}_H = \nabla_H \times \mathcal{T}\mathbf{r} = -\hat{\phi}\frac{\partial \mathcal{T}}{\partial \theta}, \tag{A9}$$

where $\mathcal{T}$ is expanded in terms of Legendre polynomials $P_l^0(\cos\theta)$ as

$$\mathcal{T} = \sum_{l=odd} t_l^0 P_l^0(\cos\theta). \tag{A10}$$

[52] The vector $\mathbf{q}$ can then be written in terms of a vector $\mathbf{t}$ containing the torsional oscillation coefficients t_l^0,

$$\mathbf{q} = \mathbf{R} \cdot \mathbf{t}, \tag{A11}$$

where the elements of matrix $\mathbf{R}$ are determined by spherical transform. Defining

$$\boldsymbol{\alpha}^T = \mathbf{k}^T \cdot \mathbf{R}, \tag{A12}$$

the axial torque is given by

$$\Gamma_z = r_f^4 G \boldsymbol{\alpha}^T \cdot \mathbf{t}, \tag{A13}$$

[53] In the formalism of torsional oscillation normal modes we need the torque at the CMB to be expressed in the form

$$\Gamma_z = \int_0^{r_f} \mathcal{F}_m(s)\left[u_f(s) - u_m\right] ds, \tag{A14}$$

where $s = r_f \sin\theta$ is the cylindrical radius and u_m and $u_f(s)$ are, respectively, the angular velocity of the mantle and the cylindrical surface of radius s in the fluid core. We can write the torque in (A13) in the form of (A14) using the definition of the coefficients t_l^0

$$t_l^0 = -\frac{2l+1}{2l(l+1)} \int_0^\pi \left(\frac{\partial}{\partial\theta} P_l^0(\cos\theta)\right) v_\phi(\theta) \sin\theta \, d\theta, \tag{A15}$$

where $v_\phi \, \hat{\phi} = \mathbf{v}_H = s[u_f(s) - u_m] \, \hat{\phi}$. In practice, we evaluate a discretized version of the torque in (A14),

$$\Gamma_z = \sum_j \mathcal{F}_m(s_j)\left[u_f(s_j) - u_m\right] \Delta s, \tag{A16}$$

where s_j is the central radius of a cylinder with finite thickness Δs and $u_f(s_j)$ is its rigid angular velocity. The discrete kernel $\mathcal{F}_m(s_j)$ depends on the magnetic field morphology at the CMB; because the field can vary significantly over the cylinder thickness Δs, especially for cylinders with $s \sim r_f$, we take its average value over the cylinder

$$\mathcal{F}_m(s_j) = \frac{1}{\Delta s} \int_{s_j - \Delta s/2}^{s_j + \Delta s/2} \mathcal{F}_m(s) ds. \tag{A17}$$

[54] Using (A15) in (A13), the torque can written in the form of (A16) with the kernel $\mathcal{F}_m(s_j)$ defined as

$$\mathcal{F}_m(s_j) = \frac{r_f^5 G}{\Delta s} \, \boldsymbol{\alpha}^T \cdot \int_{\theta_1}^{\theta_2} \tilde{\mathbf{p}} \, \sin^2\theta \, d\theta, \tag{A18}$$

where

$$\theta_1 = \arcsin\left(\frac{s_j}{r_f} - \frac{\Delta s}{2r_f}\right), \tag{A19}$$

$$\theta_2 = \arcsin\left(\frac{s_j}{r_f} + \frac{\Delta s}{2r_f}\right), \tag{A20}$$

and the elements of vector $\tilde{\mathbf{p}}$ are

$$\tilde{p}_l = -\frac{2l+1}{l(l+1)}\left(\frac{\partial}{\partial\theta} P_l^0(\cos\theta)\right), \; l = \text{odd}. \tag{A21}$$

The integral over θ in (A18) is solved numerically by Gauss-Legendre quadrature.

[55] **Acknowledgments.** We gratefully acknowledge constructive reviews by Richard Holme and Andy Jackson which improved this paper significantly. This work was completed while Mathieu Dumberry was supported by a NERC postdoctoral fellowship of the United Kingdom. Jon Mound was supported by NSF Award EAR-0337579 for a part of this work.

References

Anufriyev, A. P., and S. I. Braginsky (1977), Influence of irregularities of the boundary of the earth's core on fluid velocity and the magnetic field III, *Geomagn. Aeron.*, *17*, 492–496.

Braginsky, S. I. (1970), Torsional magnetohydrodynamic vibrations in the Earth's core and variations in day length, *Geomagn. Aeron.*, *10*, 1–10.

Buffett, B. A. (1992), Constraints on magnetic energy and mantle conductivity from the forced nutations of the Earth, *J. Geophys. Res.*, *97*, 19,581–19,597.

Buffett, B. A. (1996), Gravitational oscillations in the length of the day, *Geophys. Res. Lett.*, *23*, 2279–2282.

Buffett, B. A. (1998), Free oscillations in the length of day: inferences on physical properties near the core-mantle boundary, in *The core-mantle boundary region, Geodynamics series*, vol. 28, edited by M. Gurnis, M. E. Wysession, E. Knittle, and B. A. Buffett, pp. 153–165, AGU Geophysical Monograph, Washington, DC.

Buffett, B. A., P. M. Mathews, and T. A. Herring (2002), Modeling of nutation-precession: Effects of electromagnetic coupling, *J. Geophys. Res.*, *107*(B4), 2070, doi:10.1029/2001JB000056.

Bullard, E. C., C. Freedman, H. Gellman, and J. Nixon (1950), The westward drift of the Earth's magnetic field, *Philos. Trans. R. Soc. A*, *243*, 67–92.

Deleplace, B., and P. Cardin (2006), Viscomagnetic torque at the core mantle boundary, *Geophys. J. Int.*, *167*, 557–566.

Edmonds, A. R. (1960), *Angular momentum in quantum mechanics*, Princeton University Press, New Jersey.

Gubbins, D., and P. H. Roberts (1987), Magnetohydrodynamics of the Earth's core, in *Geomagnetism*, vol. 2, edited by J. A. Jacobs, pp. 1–184, Academic Press, London.

Hide, R. (1969), Interaction between the Earth's liquid core and solid mantle, *Nature*, *222*, 1055–1056.

Hide, R., D. H. Boggs, and J. O. Dickey (2000), Angular momentum fluctuations within the Earth's liquid core and torsional oscillations of the core-mantle system, *Geophys. J. Int.*, *143*, 777–786.

Holme, R. (1998), Electromagnetic core-mantle coupling-I. Explaining decadal changes in the length of day, *Geophys. J. Int.*, *132*, 167–180.

Holme, R. (1998b), Electromagnetic core-mantle coupling II: Probing deep mantle conductance, in *The core-mantle boundary region, Geodynamics series*, vol. 28, edited by M. Gurnis, M. E. Wysession, E. Knittle, and B. A. Buffett, pp. 139–152, AGU Geophysical Monograph, Washington, DC.

Holme, R. (2000), Electromagnetic core-mantle coupling III. Laterally varying mantle conductance, *Phys. Earth Planet. Inter.*, *117*, 329–344.

Jackson, A., J. Bloxham, and D. Gubbins (1993), Time-dependent flow at the core surface and conservation of angular momentum in the coupled core-mantle system, in *Dynamics of the Earth's deep interior and Earth rotation*, vol. 72, edited by J.-L. Le Mouël, D. E. Smylie, and T. Herring, pp. 97–107, AGU Geophysical Monograph, Washington, DC.

Jackson, A., A. R. T. Jonkers, and M. R. Walker (2000), Four centuries of geomagnetic secular variation from historical records, *Philos. Trans. R. Soc. A*, *358*, 957–990.

Jault, D., and J.-L. Le Mouël (1989), The topographic torque associated with a tangentially geostrophic motion at the core surface and inferences on the flow inside the core, *Geophys. Astrophys. Fluid Dyn.*, *48*, 273–296.

Jault, D., C. Gire, and J.-L. Le Mouël (1988), Westward drift, core motions and exchanges of angular momentum between core and mantle, *Nature*, *333*, 353–356.

Lowes, F. J. (1974), Spatial power spectrum of the main geomagnetic field, and extrapolation to the core, *Geophys. J. R. Astron. Soc.*, *36*, 717–730.

Mathews, P. M., and J. Guo (2005), Viscoelectromagnetic coupling in precessio-nutation theory, *J. Geophys. Res.*, *110*, B02402, doi:10.1029/2003JB002915.

Mathews, P. M., T. A. Herring, and B. A. Buffett (2002), Modeling of nutations and precession: New nutation series for nonrigid Earth and insights into the Earth's interior, *J. Geophys. Res.*, *107*(B4), 2068, doi:10.1029/2004JB000390.

Mauersberger, P. (1956), Das mittel der energiedichte des geomagnetischen hauptfeldes an der erdoberfläche und seine säkulare, *Gerlands Beitr. Geophys.*, *65*, 207–215.

Mound, J. E., and B. A. Buffett (2003), Interannual oscillations in the length of day: implications for the structure of mantle and core, *J. Geophys. Res.*, *108*(B7), 2334, doi:10.1029/2002JB002054.

Mound, J. E., and B. A. Buffett (2005), Mechanisms of core-mantle angular momentum exchange and the observed spectral properties of torsional oscillations, *J. Geophys. Res.*, *110*, B08103, doi:10.1029/2004JB003555.

Pais, A., and G. Hulot (2000), Length of day decade variations, torsional oscillations and inner core superrotation: Evidence from recovered core surface zonal flows, *Phys. Earth Planet. Inter.*, *118*, 291–316.

Palmer, A., and D. Smylie (2005), VLBI observations of free core nutations and viscosity at the top of the core, *Phys. Earth Planet. Inter.*, *148*, 285–301.

Rochester, M. G. (1960), Geomagnetic westward drift and irregularities in the Earth's rotation, *Philos. Trans. R. Soc. A*, *252*, 531–555.

Runcorn, S. K. (1955), The electrical conductivity of the Earth's mantle, *Trans. Am. Geophys. Union*, *36*, 191–198.

Stix, M., and P. H. Roberts (1984), Time-dependent electromagnetic core-mantle coupling, *Phys. Earth Planet. Inter.*, *36*, 49–60.

Taylor, J. B. (1963), The magneto-hydrodynamics of a rotating fluid and the Earth's dynamo problem, *Proc. R. Soc. A*, *274*, 274–283.

Zatman, S., and J. Bloxham (1997), Torsional oscillations and the magnetic field within the Earth's core, *Nature*, *388*, 760–763.

M. Dumberry, Department of Physics, University of Alberta, Edmonton, T6G 2G7, Canada. (dumberry@ualberta.ca)

J. E. Mound, School of Earth and Environment, University of Leeds, Leeds, LS2 9JT, UK. (j.mound@see.leeds.ac.uk)